

UNCORRELATED MEASUREMENTS OF THE COSMIC EXPANSION HISTORY AND DARK ENERGY FROM SUPERNOVAE

Yun Wang¹, and Max Tegmark^{2,3}

Draft version November 15, 2019

ABSTRACT

We present a method for measuring the cosmic expansion history $H(z)$ in uncorrelated redshift bins, and apply it to current and simulated type Ia supernova data assuming spatial flatness. If the matter density parameter Ω_m can be accurately measured from other data, then the dark energy density history $X(z) = \chi(z) - \chi(0)$ can trivially be derived from this expansion history $H(z)$. In contrast to customary "black box" parameter fitting, our method is transparent and easy to interpret: the measurement of $H(z)$ ¹ in a redshift bin is simply a linear combination of the measured comoving distances for supernovae in that bin, making it obvious how systematic errors propagate from input to output.

We find the Riess et al. (2004) "gold" sample to be consistent with the "vanilla" concordance model where the dark energy is a cosmological constant. We compare two mission concepts for the NASA/DOE Joint Dark Energy Mission (JDEM), the Joint Efficient Dark-energy Investigation (JEDI), and the Supernova Acceleration Probe (SNAP), using simulated data including the effect of weak lensing (based on numerical simulations) and a systematic bias from K -corrections. Estimating $H(z)$ in seven uncorrelated redshift bins, we find that both provide dramatic improvements over current data: JEDI can measure $H(z)$ to about 10% accuracy and SNAP to 30-40% accuracy.

1. introduction

Observational data on type Ia supernovae (SNe Ia) indicate that the expansion of our universe is accelerating (Riess et al. 1998; Perlmutter et al. 1999). This can be explained by the presence of dark energy. Various dark energy models have been considered, e.g. scalar fields (Freese et al. 1987; Linde 1987; Peebles & Ratra 1988; Wetterich 1988; Frieman et al. 1995; Caldwell, Dave & Steinhardt 1998) and modified gravity (Parker & Raval 1999; Boisseau et al. 2000; De Laix 2001; Mersini, Bastero-Gil, & Kanti 2001; Freese & Lewis 2002; Carroll et al. 2004) | see Padmanabhan (2003) and Peebles & Ratra (2003) for recent reviews.

Although current data seem consistent with a cosmological constant (e.g., Choudhury & Padmanabhan (2004); Chen & Ratra (2004); Daly & Djorgovski (2004); Dicus & Repko (2004); Hannestad & Mortsell (2004); Simon, Verde, & Jimenez (2004); Wang & Tegmark (2004)), the uncertainties are large and more exotic models are not ruled out (e.g., Alam, Sahni, & Starobinsky (2004); Capozziello, Cardone, & Francaviglia (2004); Huterer & Cooray (2004); Feng et al. (2004); Wang et al. (2004a)). To uncover the nature of dark energy, and differentiate among various dark energy models, it is important that we extract dark energy constraints in a model-independent manner (Wang & Gamavich 2001; Wang & Lovelace 2001; Wang & Freese 2004). The perils of model assumptions and simplified parameterization of dark energy have been shown in Maor, Brustein, & Steinhardt (2002); Wang & Tegmark (2004); Bassett, Corasaniti, & Kunz (2004).

Throughout this paper, we assume spatial flatness as motivated by inflation. Calibrated cosmological standard candles such as SNe Ia measure the luminosity distance

$d_L(z) = (1+z)r(z)$, where the comoving distance

$$r(z) = \int_0^z \frac{dz^0}{H(z^0)} = H^{-1} \int_0^z \frac{dz^0}{h(z^0)} \quad (1)$$

where $c = 1$, $H = 100 \text{ km s}^{-1} \text{ Mpc}^{-1}$ and

$$h(z) \equiv H(z) = h(0) \Omega_m (1+z)^3 + \chi X(z)^{1/2}; \quad (2)$$

with $X(z) = \chi(z) - \chi(0)$ denoting the dark energy density function. Determining if and (if so how) the dark energy density $X(z)$ depends on cosmic time is the main observational goal in the current quest to illuminating the nature of dark energy. Given a precise measurement of the matter density fraction Ω_m (from galaxy redshift surveys, for example), the dark energy density function $X(z)$ can be trivially determined from $H(z)$ via equation (2).

Numerous methods for this have been developed and applied in the recent literature, either by parameterizing $X(z)$ in terms of an equation of state and perhaps additional parameters or by aiming for more model-independent constraints (e.g., Wang & Tegmark (2004)). Equation (1) shows that the data directly constrain the cosmic expansion history $H(z)$, and the information-theoretically minimal error bars on $H(z)$ from supernovae were derived in Tegmark (2001) using a Fisher matrix approach. Yet no method for doing this in practice has been found other than the "black box" approach of parameterizing $H(z)$ somehow and fitting to the data. Ideally one would like to measure $H(z)$ in many redshift bins with uncorrelated error bars, but Tegmark (2001) found that parameterized fits tend to yield broad and difficult-to-interpret window functions, i.e., the measurement in a given redshift bin depended also on supernova data far outside that redshift range. Huterer & Cooray (2004) strengthened this conclusion by showing that uncorrelated measurements of the expansion history

¹ Department of Physics & Astronomy, University of Oklahoma, 440 W Brooks St., Norman, OK 73019; email: wang@nhn.ou.edu² Dept. of Physics, Massachusetts Institute of Technology, Cambridge, MA 02139, USA; tegmark@mit.edu³ Dept. of Physics, University of Pennsylvania, Philadelphia, PA 19104, USA

(computed by diagonalizing the Fisher matrix) tended to probe a broad redshift range.

The purpose of the present paper is to solve this problem, presenting a method giving uncorrelated measurements of the expansion history in arbitrary redshift bins. We will see that this method is both easy to implement and easy to interpret. We describe our method in Sec. 2 and the simulated data in Sec. 3. We present our results in Sec. 4 and discuss our conclusions in Sec. 5.

2. method

Assuming that the redshifts of SNe Ia are accurately measured, we can neglect redshift uncertainties, and simply treat the measured comoving distances $r(z_i)$ to the supernovae as the observables. In terms of r_0 , the distance modulus of SNe Ia, we have

$$\frac{r(z)}{1 \text{ Mpc}} = \frac{1}{2997.9(1+z)} 10^{0.55} : \quad (3)$$

Let us write the comoving distance measured from the i^{th} SNe Ia as

$$r_i = r(z_i) + n_i; \quad (4)$$

where the noise vector satisfies $\langle n_i n_j \rangle = \delta_{ij}$.

2.1. Transforming to measurements of $H(z)^1$

As a first step in our method, we sort the supernovae by increasing redshift $z_1 < z_2 < \dots$, and define the quantities

$$x_i = \frac{r_{i+1} - r_i}{z_{i+1} - z_i} = \frac{\frac{R_{z_{i+1}} - R_{z_i}}{z_{i+1} - z_i} \frac{dz^0}{H(z^0)} + n_{i+1} - n_i}{z_{i+1} - z_i} = \bar{f}_i + (n_{i+1} - n_i) = z_i; \quad (5)$$

where $\bar{f}_i = (z_{i+1} - z_i)^{-1} \int_{z_i}^{z_{i+1}} H(z) dz$ is the average of $H(z)$ over the redshift range (z_i, z_{i+1}) . Note that x_i gives an unbiased estimate of the average of $H(z)$ in the redshift bin, since $\langle x_i \rangle = \bar{f}_i$, so the quantities x_i are direct (but noisy) probes of the cosmic expansion history. Assembling the numbers x_i into a vector x , its covariance matrix $N = \langle x x^T \rangle - \langle x \rangle \langle x^T \rangle$ is tridiagonal, satisfying $N_{ij} = 0$ except for the following cases:

$$N_{i,i-1} = \frac{z_{i+1}^2 - z_i^2}{z_{i+1} - z_i}; \\ N_{i,i} = \frac{z_i^2 + z_{i+1}^2}{z_i^2}; \\ N_{i,i+1} = \frac{z_{i+1}^2 - z_i^2}{z_{i+1} - z_i}; \quad (6)$$

The new data vector x clearly retains all the cosmological information from the original data set (the comoving distance measurements r_i), since the latter can trivially be recovered from x up to an overall constant offset set by inverting equation (5). In summary, the transformed data vector x expresses the SNe Ia information as a large number of unbiased but noisy measurements of the cosmic expansion history in very fine redshift bins, corresponding to the redshift separations between neighboring supernovae.

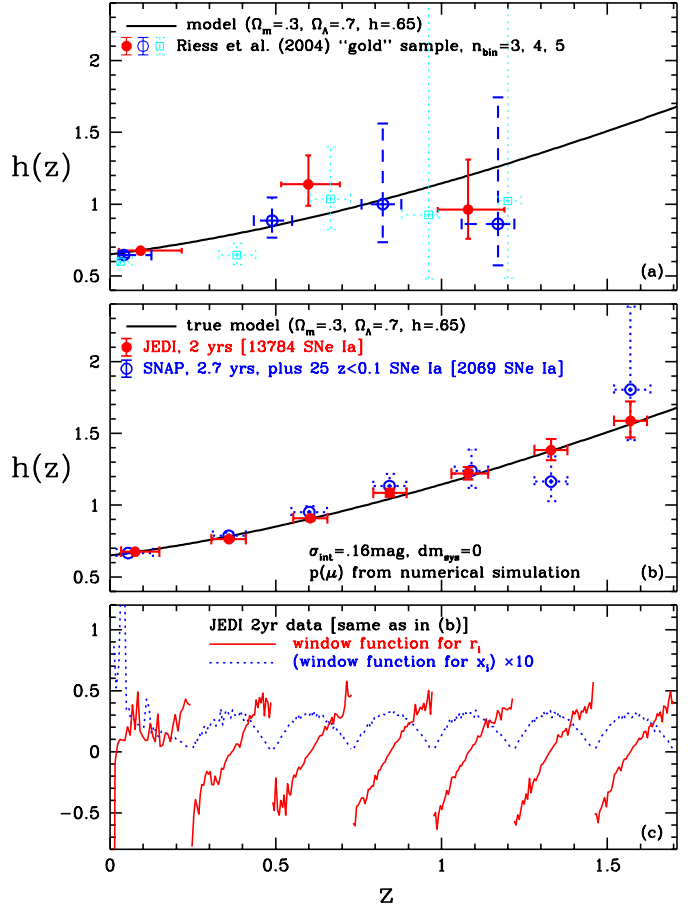


Fig. 1. The cosmic expansion history (the dimensionless Hubble parameter $h(z)$) is measured in uncorrelated redshift bins from the Riess et al. (2004) "gold" sample (top panel) and from simulated future data (middle panel) for the NASA/JDEM mission concepts JED I (solid lines) and SNAP (dotted lines). The measured $h(z)^1$ in a given redshift bin is simply the sum of the comoving supernova distances in that bin, weighted by the corresponding solid curve in the bottom panel, which roughly speaking subtracts more nearby supernovae from more distant ones.

2.2. Averaging in redshift bins

The second step in our method is to average these noisy measurements x into minimum-variance measurements y_i of the expansion history in some given redshift bins. For instance, the middle panel of Figure 1 shows an example with seven bins, $i = 1, \dots, 7$. Let the vector x^i denote the piece of the x -vector corresponding to the i^{th} bin, and let N_i denote the corresponding covariance matrix. Our weighted average y_i can then be written

$$y_i = w^i \cdot \bar{x} \quad (7)$$

for some weight vector w^i whose components sum to unity, i.e., $\sum_j w_j^i = 1$ or equivalently $e^T w^i = 1$, where e is a vector containing all ones; $e_i = 1$. To find the best weight vector w^i , we minimize the variance

$$y_i^2 = \bar{y}_i^2 - \bar{y}_i^2 \cdot \bar{y}_i^2 = w^i \cdot N_i \cdot w^i \quad (8)$$

subject to the constraint that the weights add up to unity, i.e., $e^T w^i = 1$. This constrained minimization problem is readily solved with the Lagrange multiplier method,

giving

$$w^i = \frac{N_i^{-1} e}{e^t N_i^{-1} e}; \quad (9)$$

and substituting this back into equation (8) gives the size of the corresponding error bar:

$$y_i = e^t N_i^{-1} e^{-1/2}; \quad (10)$$

The bottom panel in Figure 1 shows the seven weight vectors w^i (dotted) corresponding to the seven measurements y_i in the middle panel (solid points). We will also refer to the weight vectors as window functions, since they show the contributions to our measurements from different redshifts. Note that each window function vanishes outside its redshift bin, and that all seven of them share a characteristic bump shape roughly corresponding to an upside-down parabola vanishing at the bin endpoints. To illustrate the z -range that each measurement probes, we follow Tegmark & Zaldarriaga (2002) and plot it at the median of the window function w with horizontal bars ranging from the 20th to the 80th percentile. For a bin with width z centered at a redshift z , this corresponds to plotting $z \pm 0.213 z$ if the window is well approximated by an upside-down parabola.

Since the measurements y_i are linear combinations of the x_i which are in turn linear combinations of the r_i , we can also reexpress our measurements directly as linear combinations of the original supernova comoving distances:

$$y_i = \sum_j w_j^i r_j; \quad (11)$$

where the new window functions

$$w_j^i = \frac{w_{j-1}^i}{z_{j-1}} - \frac{w_j^i}{z_j} \quad (12)$$

would be essentially the negative derivative of the old window functions if all redshift intervals were the same. These new window functions are also plotted in the bottom panel of Figure 1 (solid "saw tooth" curves), and are seen to be roughly linear (as expected for a parabola derivative), effectively subtracting supernovae at the near end of the bin from those at the far end.

A major advantage of this method is its transparency and simplicity. If one fits some parameterized model of $H(z)$ to the SN Ia data by maximizing a likelihood function, then the resulting parameter estimates will be some complicated (and generically nonlinear) functions of all the data points r_j . In contrast, the measurement y_5 in our 5th bin in Figure 1 (middle panel) is simply a linear combination of the comoving distance measurements for the supernovae in the 5th bin ($1.0 < z_i < 1.4$) as defined by the 5th window function in the bottom panel, so it is completely clear how each particular supernova affects the final result. In particular, the supernovae outside of this redshift range do not affect the measurement at all.

We conclude this section by discussing some details useful for the reader interested in applying our method in practice.

2.3. Creating uncorrelated redshift bins

⁴ A Fortran code that uses flux-averaging statistics to compute the likelihood of an arbitrary dark energy model (given the SN Ia data from Riess et al. (2004)) can be found at <http://www.nhn.ou.edu/~wang/SNcode/>.

⁵ This is consistent with the findings of Wang & Tegmark (2004).

We suggest discarding those x_i straddling neighboring bins, i.e., whose two supernovae fall on either side of a bin boundary. For say 7 bins there are only 6 such numbers, so this involves a rather negligible loss. The advantage is that it ensures that two measurements y_i and y_j have completely uncorrelated error bars if $i \neq j$, since their window functions w have no supernovae in common.

2.4. Flux averaging

To minimize the bias in the $H(z)$ measurement due to weak lensing, we use flux-averaging (Wang 2000b; Wang & Mukherjee 2004)⁴. Specifically, we compress the full supernova data set r_i into a smaller number of flux-averaged supernovae assigned to the mean redshift in each of a large number of bins of width z . We use $z = 0.05$ for the current data and $z = 0.005$ for the simulated data. Note that since we have assumed a Gaussian distribution in the magnitudes of SN Ia at peak brightness, flux-averaging leads to a tiny bias of $\sqrt{\ln 10} = 5$ mag (Wang 2000a). We have removed this tiny bias in the data analysis.

As a side effect, this averaging in narrow bins makes the denominators z_i roughly equal in equation (5), so that the only noticeable source of wiggles in the window functions in Figure 1 (bottom) is Poisson noise, i.e., that some of these narrow bins contain more supernovae than others. The method of course works without this averaging step as well. In that case, the window functions w wobble substantially because of variations in the redshift spacing between supernovae, since very little weight is given to x_i if z_i happens to be tiny. However, we find that the supernova window functions w remain rather smooth and well-behaved functions of redshift, as expected | two supernovae very close together with the same noise level σ_i automatically get the same weight. This means that our method effectively averages such similar redshift supernovae anyway, even if we do not do so by hand ahead of time. The difference between flux averaging and this automatic averaging is simply that we average their fluxes rather than their comoving distances | these two types of averaging are not equivalent since the flux is a nonlinear function of the comoving distance.

3. results

Figure 1 shows the results of applying our method to both real data (top panel) and simulated data (middle panel), with the dimensionless expansion rate of the Universe $H(z)$ measured in between three and seven uncorrelated redshift bins.

The top panel uses the "gold" set of 157 SN Ia published by Riess et al. (2004). The error bars are seen to be rather large, and consistent with a simple $H(z) = H_0 z$ concordance model where the dark energy is a cosmological constant.⁵ As was shown in Tegmark (2002) using information theory, the relative error bars on the cosmic expansion history $H(z)$ scale as

$$\frac{H}{H_0} / \frac{N^{1/2}}{z^{3/2}}; \quad (13)$$

for N supernovae with noise σ . Here z is the width of the redshift bins used, so one pays a great price for narrower bins: halving the bin size requires eight times as

many supernovae. The origin of this $(z)^{3/2}$ -scaling is intuitively clear: the noise averages down as $(z)^{1/2}$, and there is an additional factor of $(z)^{1/2}$ from effectively taking the derivative of the data to recover $H(z)^{1/2}$ from the integral in equation (5)⁶. The bottom panel in Figure 1 shows that the method effectively estimates this derivative by subtracting supernovae at the near end of the bin from those at the far end of the bin and dividing by z .

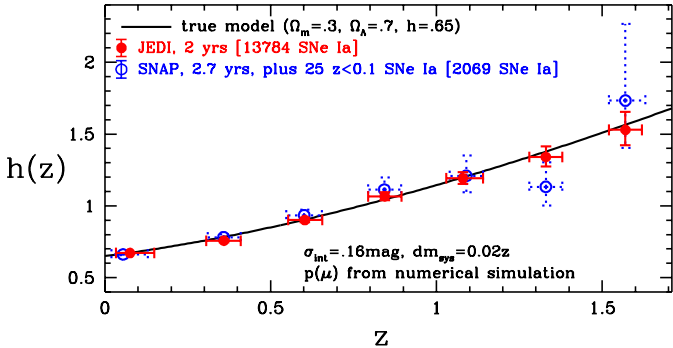


Fig. 2.| Same as Fig. 1(b), but with a systematic bias of $dm_{sys} = 0.02z$ from K-correction uncertainties added in addition to lensing noise computed from numerical simulations (Barber 2003).

This means that for accurately measuring $H(z)$ and thereby the density history of the dark energy, numbers really do matter. For example, in order to measure the dark energy density function to 10% accuracy in seven uncorrelated redshift bins as in the middle panel of Figure 1 (with $z = 0.243$), we need to have around 14,000 SNe Ia. We have simulated SNe Ia data by placing supernovae at random redshifts, with the number of SNe Ia per 0.1 redshift interval given by a distribution. The intrinsic brightness of each SNe Ia at peak brightness is drawn from a Gaussian distribution with a dispersion of $\sigma_{int} = 0.16$ mag. As the fiducial cosmological model, we used a flat universe with $\Omega_m = 0.3$.

We compare two mission concepts for the NASA/DOE Joint Dark Energy Mission (JDEM): the Joint Efficient Dark-energy Investigation (JEDI) (Wang et al. 2004b) and the Supernova Acceleration Probe (SNAP) (Alldering et al. 2004). For JEDI (solid lines in Figure 1), the number of SNe Ia per 0.1 redshift interval is obtained by fitting the measured SNe Ia rate as function of redshift (Cappellaro, Evans, & Turatto 1999; Hardin et al. 2000; Dahmen et al. 2004) to a model assuming a conservative delay time between star formation and SNe Ia explosion of 3.5 G yrs. For SNAP (dotted lines in Figure 1), the number of SNe Ia per 0.1 redshift interval is taken from Figure 9 in Alldering et al. (2004).

We consider two kinds of SNe Ia systematic uncertainties: weak lensing due to intervening matter and a systematic bias due to K-corrections. We include the weak lensing effect by assigning a magnification drawn from a probability distribution $p(\mu)$, extracted using an improved version of the Universal Probability Distribution Function (UPDF) method (Wang, Holz, & Munshi 2002)

⁶ Analogous estimates of the equation of state $w(z)$ have a painful $(z)^{5/2}$ -scaling, since they effectively involve taking the second derivative

from the numerical simulations of weak lensing by Barber (2003). The total uncertainty in each SNe Ia data point is $\sigma_{int}^2 + \sigma_{lens}^2$, with $\sigma_{lens}(z)$ extracted from Barber (2003):

$$\sigma_{lens}(z) = 0.00311 + 0.08687z - 0.00950z^2 \quad (14)$$

We consider a systematic bias of $dm_{sys} = 0.02z$ due to K-corrections following Wang & Gamavich (2001).

We did not include the systematic bias due to K-corrections in Fig. 1, in order to compare the real data (Riess et al. 2004) and simulated data on an equal footing.

In Fig. 2, we show the effect of adding the systematic bias due to K-corrections in addition to the weak lensing noise. Comparing Fig. 2 with Fig. 1(b), we see that the systematic bias does not have a significant effect on the uncorrelated estimates of $H(z)$. This is because our method effectively reduces a global systematic bias into a local bias with a much smaller amplitude (see Sec. 2).

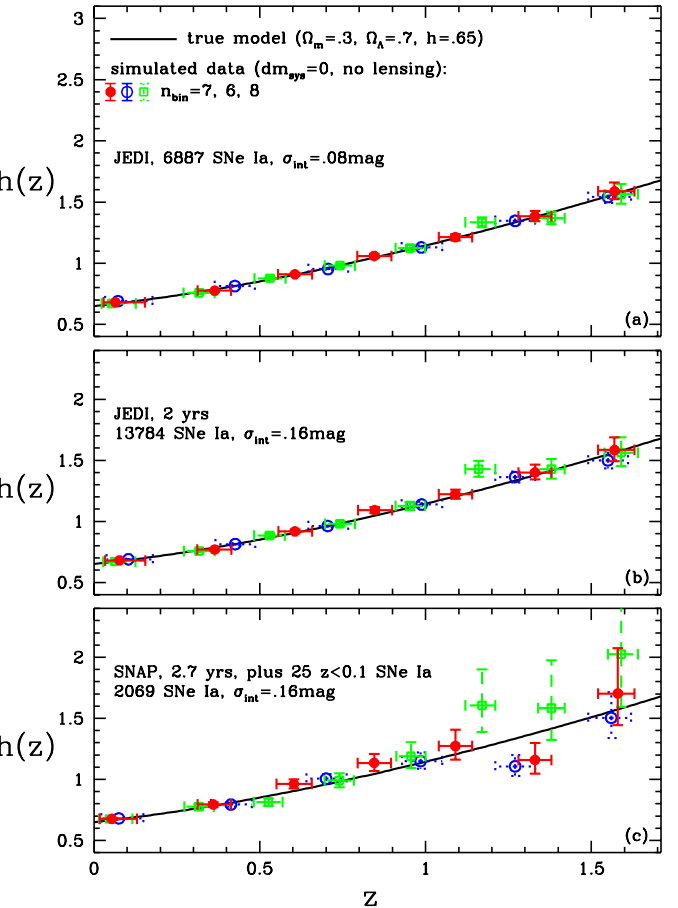


Fig. 3.| How the recovery of the cosmological expansion history $h(z)$ depends on the number of redshift bins, assuming no systematic bias and no lensing. (a) Half of JEDI data, with a reduced intrinsic scatter of $\sigma_{int} = 0.08$ mag. (b) All of JEDI data, with $\sigma_{int} = 0.16$ mag. (c) All of SNAP data (plus 25 SNe Ia at $z < 0.1$), with $\sigma_{int} = 0.16$ mag.

Figure 3 shows the recovery of the cosmological expansion history $h(z)$ depends on the number of redshift bins (6, 7 and 8), assuming no systematic bias and no lensing, and

agrees well with the theoretical (z)³⁼² scaling. Contrasting current and future data with roughly the same redshift binsize for both ($n_{\text{bin}} = 5$ for current data, and $n_{\text{bin}} = 7$ for the simulated data) shows that JED I shrinks the error bars by more than an order of magnitude, so the potential in provenent with a successful JDEM would be dramatic.

Figure 3 compares three different data sets: (a) Half of the JED I data, with a reduced intrinsic scatter of $\text{int} = 0.08$ mag from sub-typing. (b) All the JED I data, with $\text{int} = 0.16$ mag. (c) All the SNAP data (plus 25 SNe Ia at $z < 0.1$), with $\text{int} = 0.16$ mag.

Note that since the measured quantity $h(z)$ ¹ typically is not a straight line, the measured average of this curve over a redshift bin will generally lie either slightly above or below the curve at the bin center. Figure 1 shows that this bias is substantially smaller than the measurement uncertainties, since $h(z)$ and $h(z)$ ¹ are rather well approximated by straight lines over the narrow redshift bins that we have used.

A second caveat when interpreting our figures is that the absolute calibration of SNe Ia is not perfectly known | changing this simply corresponds to multiplying the function $h(z)$ by a constant, i.e., to scaling the measured curve vertically.

4. discussion

We have presented a method for measuring the cosmic expansion history $H(z)$ in uncorrelated redshift bins, and applied it to current and simulated supernova Ia data assuming spatial flatness. Whereas previously proposed approaches involve "black box" parameter fitting, this method is transparent and simple to interpret: the measurement of $H(z)$ ¹ in a redshift bin is simply a linear combination of the measured comoving distances for supernovae in that bin, with weights that roughly correspond to subtracting closer supernovae from more distant ones. Such transparency is particularly helpful for understanding how systematic errors in the input affect the output. For instance, a constant systematic dimming throughout a redshift bin will leave that measurement unaffected.

This method is useful for understanding the nature of dark energy, since the dark energy density history follows from this expansion history $H(z)$ if the matter density parameter m can be accurately measured from other data (e.g., the cosmic microwave background, galaxy clustering and gravitational lensing). We found the Riess et al. (2004) "gold" sample to be consistent with the "vanilla" concordance model where the dark energy is a cosmological constant, but that much larger numbers of supernovae

are needed for true precision tests of the nature of dark energy.

Looking towards the future, we compare two mission concepts for the NASA/DOE Joint Dark Energy Mission (JDEM), the Joint Einstein Dark-energy Investigation (JEDI) and the Supernova Acceleration Probe (SNAP), using simulated data including the effect of weak lensing and bias from K-corrections. Estimating $H(z)$ in seven uncorrelated redshift bins, we find that both provide dramatic improvements over the present state-of-the art: JEDI can measure $H(z)$ to about 10% accuracy, and SNAP can measure $H(z)$ to 30–40% accuracy (Figure 1).

Our results show that numbers do matter. For example, in order to measure the cosmic expansion history to 10% accuracy in seven uncorrelated redshift bins (with $z = 0.243$), we need to have around 14,000 SNe Ia (as expected from two years of JEDI data), assuming a dispersion of 0.16 magnitudes in SN Ia peak brightness (Figure 1). Estimating $H(z)$ to 10% in smaller uncorrelated redshift bins will require an even larger number of SNe Ia (if a significant reduction in intrinsic dispersion is not assumed for a sizable fraction of the SNe Ia), which will be difficult to obtain in a feasible two-year space mission. Also, $H(z)$ estimated in $z = 0.243$ redshift bins (for $0 < z < 1.7$) to 10% accuracy will give us a powerful means to differentiate between a cosmological constant and dark energy models which are not fine-tuned to mimic a cosmological constant. A sample with a large number of SNe Ia allows a tighter calibration of SNe Ia as standard candles and sub-typing of SNe Ia to reduce diversity. This may yield a smaller set of SNe Ia with substantially smaller intrinsic dispersion, which can lead to more robust and stable estimates of the expansion history of the universe (Figure 3). If the subtyping works well in reducing the intrinsic dispersion of SNe Ia, we can expect to be able to measure $H(z)$ in more than seven redshift bins to 10% accuracy for $0 < z < 1.7$ (Figure 3).

A precise measurement of the cosmic expansion history as a free function of cosmic time to 10% accuracy would represent a dramatic improvement in our knowledge about dark energy. Our results suggest that a JDEM can achieve this scientific goal.

Acknowledgments We thank David Branch and Peter Garnavich for helpful comments. This work was supported by NSF CAREER grants AST-0094335 (YW) and AST-0134999 (MT), NASA grant NAG 5-11099 and fellowships from the David and Lucile Packard Foundation and the Cottrell Foundation (MT).

REFERENCES

Alam, U., Sahni, V., & Starobinsky, A. A. 2004, *JCAP*, 0406, 008,
Aldering, G., et al., *astro-ph/0405232*
Barber, A. J., et al. 2000, *MNRAS*, 319, 267
Barber, A. J. 2003, private communication
Bassett, B. A., Corasaniti, P. S., Kunz, M. 2004, *Astrophys.J.* 617, L1–L4
Boisseau, B., Eposito-Farese, G., Polarski, D. & Starobinsky, A. A. 2000, *Phys. Rev. Lett.*, 85, 2236
Caldwell, R., D'Ave, R., & Steinhardt, P. J., 1998, *PRL*, 80, 1582
Cappellaro, E., Evans, R. J., & Turatto, M. 1999, *A & A*, 351, 459
Capozziello, S., Cardone, V. F., & Francaviglia, M. 2004, *astro-ph/0410135*
Carroll, S. M., de Felice, A., Duvvuri, V., Easson, D. A., Trodden, M. & Turner, M. S., *astro-ph/0410031*
Chen, G., & Ratra, B. 2004, *Astrophys.J.* 612, L1
Choudhury, T. R., & Padmanabhan, T. 2004, *astro-ph/0311622*, A & A in press
Dahlen, T., et al. 2004, *ApJ*, 613, 189
Daly, R. A., & Djorgovski, S. G. 2004, *ApJ*, 612, 652
De la ayet, C., 2001, *Phys. Lett. B*, 502, 199
Dicus, D. A., & Repko, W. W. 2004, *Phys. Rev. D* 70, 083527
Feng, B., Li, M., Piao, Y.-S., Zhang, X., *astro-ph/0407432*
Freese, K., et al., 1987, *Nucl. Phys.*, B 287, 797
Freese, K., & Lew, M., 2002, *Phys. Lett. B*, 540, 1
Frieman, J. A., Hill, C. T., Stebbins, A., and Waga, I., 1995, *PRL*, 75, 2077
Hannestad, S., & Mortsell, E. 2004, *JCAP*, 0409, 001
Hardin, D., et al. 2000, *A & A*, 362, 419

Huterer, D ., & Cooray, A ., astro-ph/0404062

Linde A D ., "In ation A nd Q uantum C osm ology," in Three hundred years of gravitation, (Eds.: Haw king, S.W . and Israel, W ., Cambridge Univ. Press, 1987), 604-630.

Maor, I., Brustein, R ., & Steinhardt, P .J., 2002, PRL, 86, 6

Mersini, L., B astero-G il, M ., & K anti, P ., 2001, PRD, 64, 043508

Padmanabhan, T ., 2003, Phys. Rep., 380, 235

Parker, L ., and R ayal, A ., 1999, PRD, 60, 063512

Perlmutter, S. et al., 1999, ApJ, 517, 565

Peebles, P J E ., and R atra, B ., 1988, ApJ, 325, L17

Peebles, P J E ., & R atra, B ., 2003, Rev. Mod. Phys., 75, 559

Simon, J., Verde, L ., & Jim enez, R ., 2004, astro-ph/0412269

R iess, A . G ., et al., 1998, Astron. J., 116, 1009

R iess, A . G ., et al. 2004, ApJ, 607, 665

Tegmark, M ., 2000, Phys. Rev. D , 66, 103507

Tegmark, M ., 2002, Phys. Rev. D 66, 103507

Tegmark, M ., & Zaldarriaga, M ., 2002, Phys. Rev. D 66, 103508

W ang, Y ., 2000a, ApJ, 531, 676

W ang, Y ., 2000b, ApJ, 536, 531

W ang, Y ., K ratochvil, J.M ., Linde, A ., & Shm akova, M ., 2004a, astro-ph/0409264, JCAP in press

W ang, Y ., et al. 2004b (the JED I Team), BAAS, 36, 5, AAS205, 1328. See also <http://jedinhn.sou.edu/>.

W ang, Y ., Holz, D E ., and Munshi, D ., 2002, ApJ, 572, L15

W ang, Y ., and Freese, K ., astro-ph/0402208

W ang, Y ., and Gamavich, P ., 2001, ApJ, 552, 445

W ang, Y ., and Lovelace, G ., 2001, ApJ, 562, L115

W ang, Y ., and Mukherjee, B ., 2004, ApJ, 606, 654

W ang, Y ., & Tegmark, M ., 2004, Phys. Rev. Lett., 92, 241302

W etterich, C ., 1988, NuclPhys., B 302, 668